Effect of Radiation Exposure on the Hall-Petch Relation and Its Significance on Radiation Embrittlement in Iron and Ferritic Steels

I. Charit and K.L. Murty
North Carolina State University
Raleigh, NC 27695-7909
United States of America

ABSTRACT

Effect of neutron irradiation on grain size dependence of yield strength was investigated on pure iron (Armco Fe) from which the friction and source hardening components were derived. The results indicated decreased source hardening or unpinning coefficient following radiation exposure while the friction hardening increased with square-root of fluence. The significance of the partitioning into components lies in our ability to predict the increase in ductile-brittle transition temperature following radiation using Cottrell's brittle fracture theory. Temperature dependence of friction and source hardening terms was examined before and after radiation exposure. A low carbon mild steel was also included along with commercial steels commonly used for pressure boundary applications. Dynamic strain aging (DSA) at elevated temperatures exhibited the characteristic athermal regions accompanied by reduced ductility and toughness. Effects of neutron irradiation resulted in reduced degree of locking of the dislocations by interstitial atoms, increased temperature for the onset of serrations and lowered temperature range. Synergistic effects of DSA and radiation defects revealed apparent increases in ductility and toughness in the DSA regime following radiation exposure. The influence of low energy neutrons was investigated by comparing irradiation data with and without Cd-wrapping. The observed results were explained using radiation effects on the Hall-Petch relation.

INTRODUCTION

Ferritic steels are commonly used in fission reactors for pressure vessels, reactor support structures and steam generator housings in fast reactors. In addition, ferritic/martensitic steels are being considered for new generation nuclear power reactors considered for higher temperature operation. These materials follow the well known Hall-Petch equation relating the strength to the grain size that comprises of two components, friction hardening (σ_i) and solution hardening (σ_s):

$$\sigma_y = \sigma_i + \sigma_s = \sigma_i + \frac{k_y}{\sqrt{D}}, \tag{1}$$

where σ_s is the stress experienced by the dislocation sources due to locking by solute atmospheres, σ_i is the friction hardening representing the stress experienced by the unlocked dislocations moving through the lattice, D is the grain size and k_y represents the unpinning coefficient. The friction hardening increases following radiation exposure due to excess dislocations and other defects such as planar and volumetric defects produced due to the interaction of the high energy neutrons with the lattice. However, during irradiation at room temperature and above the interstitial impurity atoms diffuse from the solute atmospheres locking the dislocations to the radiation produced point defects such as vacancies and interstitials thereby resulting in decreased source hardening in irradiated materials. Thus the yield strength (σ_y) increases with fluence at a slightly decreased rate [1]. These aspects are very clearly noted in pure iron and low carbon mild steel while alloying elements in structural steels lead to decreased source hardening. For example, source hardening could attain equal to or slightly larger than the friction hardening for Armco Fe, it is around 10% of the friction stress for A516 steel [1]. Effects of test temperature and in particular neutron irradiation on these components are important in characterizing the radiation effects on ductile to brittle transition temperature (DBTT). It is well known that ferritic steels exhibit DBTT and neutron radiation exposure results in creased DBTT. Using Cottrell's brittle fracture theory, one can relate the changes due to temperature and irradiation to the increase in DBTT [2]:

$$\Delta DBTT = \frac{1 + \dfrac{2\Phi^2 \sigma_y}{\sigma_i}\left(\dfrac{d\sigma_s}{d\Phi}\right)}{1 + \dfrac{\sigma_y}{\sigma_s}\left(\dfrac{d\sigma_s}{dT}\right)} \Delta\sigma_i \,. \tag{2}$$

In this equation, Φ is fluence, T test temperature and $\Delta\sigma_i$ is increase in friction hardening which is expected to be proportional to the defect density that in turn increases linearly with fluence. However, it is often difficult to find data on the temperature and fluence dependence of σ_s which makes it difficult to apply for practical applications.

These materials also exhibit dynamic strain aging due to the interaction of dislocations with interstitial impurity atoms such as C and N resulting in increased work hardening and negative strain-rate-sensitivity. These phenomena lead to jerky or serrated stress-strain curves [3] which results in a precipitous drop in ductility, a phenomenon commonly referred to as *blue brittleness*. Concern arises then as to the possible addition of this brittleness to radiation embrittlement of ferritic steels [4], [5].

The extensive data base on various reactor vessel surveillance capsule programs revealed the influence of alloying elements such as Cu, Ni and P on the changes in DBTT and upper shelf energy along with the superimposed effects of radiation fluence and irradiation temperature [2]. While these factors were well established, the underlying micro-mechanisms responsible for these changes are at best speculative and various attempts in the development of these mechanisms and models were hampered by the fact that the microscopic defects and defect complexes responsible for these effects are too small to be resolvable by standard electron microscopy techniques. Ultrafine defect characterization requires advanced techniques such as field ion microscopy atom probe; small angle neutron scattering, etc and recent studies using positron annihilation spectroscopy [6] revealed that radiation-enhanced precipitation of carbides and nitrides plays a major role in radiation embrittlement of ferritic steels. These analyses imply that the elements such as Cu, Ni and P modify the kinetics of carbide precipitation thereby indirectly influencing the radiation embrittlement. These observations are strikingly different from the hither-to believed premise based on the radiation enhanced precipitation of Cu [7], [8]. These findings clearly warrant well planned research investigations on the effects of IIAs and various alloying elements on mechanical and fracture characteristics along with the superimposed radiation effects. In addition, the distinct flux rate effects noted on radiation embrittlement lead to the fact that materials exposed at lower irradiation temperatures (such as the reactor supports) may be embrittling at much higher rates than predicted from the data on pressure vessel steels which are exposed to higher energy neutrons at relatively higher temperatures. Thus the Nuclear Materials group at NCSU embarked on an extensive radiation effects program with the major objective being the characterization of the synergistic effects of DSA and radiation [1], [4], [5], [9], [10]. For an understanding of the underlying mechanisms, relatively pure Armco-iron and silicon killed mild steel [11] are used along with a number of low alloy steels with varied compositions. We present here the experimental results on Armco-Fe of varying grain sizes (50μm - 300μm), Si-killed mild steel, A516Gr70, typically used for reactor supports, and A533B, a typical pressure vessel steel. The degree of serrations and its effects on the mechanical and fracture characteristics are sensitive to the composition of the steel, and these behaviors are examined in the steels mentioned above.

The effect of low energy neutrons (Cd cut-off) on strength of these materials was examined by evaluating the specimens with and without Cd wrapping. We find distinct differences between pure iron and alloy steels which could be explained using Hall-Petch relation and the effect of radiation exposure on friction and source hardening terms.

EXPERIMENTAL ASPECTS

Table 1 lists the compositions of the iron and steels investigated here. Mild steel wires of 1 mm diameter and 38.5 mm gauge length were received from cold-drawn rimmed stock and were annealed in vacuum at 973 K. The mean grain size is 0.038 mm and the annealed samples were irradiated in high isotope flux Australian reactor (HIFAR) which is a heavy water moderated reactor at Lucas Heights, Australia. The specimens were inserted in vertical holes at different positions with varied neutron flux. With the time of irradiation being kept constant, different neutron fluences were obtained with the highest for the samples closest to the core. Irradiation temperature was maintained to be the same as that of the coolant at 353 K. The irradiated specimens were kept in lead coffins till the activity decayed for mechanical property evaluation.

Table 1. Compositions (wt.%) of Ferritic Steels

Material	C	Mn	Si	S	P	Cu	Mo	Al	Ni	Cr	V
A516	0.20	0.98	0.20	0.018	.024	0.24	0.03	0.018	0.16	0.20	0.004
A588	0.20	1.20	0.31	0.04	0.04	0.22	0.05	-	0.21	-	-
1020	0.20	0.40	0.10	0.04	0.04	-	-	-	-	-	-
Armco-Fe	0.008	0.04	0.02	0.003	0.004	-	-	-	-	-	-

Armco-iron with varied grain sizes was provided by the Defense Metallurgical Research Laboratory, India in plate form [12] and subsize tensile specimens machined from the plate were electropolished to remove the damaged layers. Four different grain sizes were studied with mean grain sizes of 50 μm, 110 μm, 190 μm and 300 μm with around 6% a variation.

Forged plates of low strength pressure vessel steels (A516 and A588) were obtained from forged plates taken at the ¼-thickness from which subsize tensile specimens were machined. In addition, 1020 steel specimens were also prepared. Tensile samples were dog-bone type with a total length of 38 mm with 12.7 mm gauge section and rectangular cross section of 2 mm wide by 1 mm thick. The grain size of the alloy steels is around 30 μm. the chemical compositions of the experimental materials are included in Table 1.

The prepared specimens were inserted in vacuum sealed quartz tubes with high purity nickel (98.98%, ^{58}Ni) wires for flux calculations. Some of the tubes were wrapped with 0.5 mm thick cadmium to filter high energy neutrons and it was estimated that 90% of thermal and epithermal neutrons were filtered. These quartz tubes with and without cadmium wrapping were placed into an aluminum fixture that had holes to accommodate the tubes arranged around its circumference. The aluminum fixture was inserted in the aluminum canister for placement in the NCSU PULSTAR reactor which is a 1 MW thermal reactor and the irradiation temperature is the same as the coolant temperature at 323 K. NaI detector was used to measure the 811 keV gamma rays emitted by the radioactive decay of ^{58}Co from the threshold reaction ^{58}Ni(n,p)^{58}Co. The fast (≥0.1 MeV] flux was calculated to be 2x10^{12} n/cm^{2}-sec and the total effective exposure times were 2.16x10^{6} seconds. The fast and thermal neutron fluences were estimated to be 2.8x10^{18} n/cm^{2} and 3.4x10^{19} n/cm^{2} respectively.

Tensile tests were performed on a closed loop hydraulic Instron machine for iron and steels while the mild steel wires were tested using a hard tensile machine at varied temperatures and applied strain-rates. The strengths were evaluated with a scatter in the data of around ± 9.5 MPa for Armco-Fe, ± 7.5 MPa for mild steel and ± 11 MPa for other steels.

EXPERIMENTAL RESULTS AND DISCUSSION

Synergistic Effects of DSA and Neutron Irradiation (Mild Steel)

Load-elongation curves for unirradiated mild steel are included in Fig. 1 at varied temperatures which clearly reveal the unstable plastic flow at temperatures greater than 363 K and below 544 K. We note jerky flow at lower temperatures while serrated deformation at higher temperatures and these are attributed to the locking of the dislocations by interstitial C and N [3], [5], [11] often referred to as dynamic strain aging (DSA). Nitrogen locking is predominant in slowly cooled materials since majority of carbon precipitates into cementite [13] while nitrogen stays in solution. At room temperature, the stress-elongation curve is smooth while at 363 K, random load drops are observed in the flow curve (jerky flow), but the Luders plateau remains largely smooth. At the lower critical temperature (413 K), random stress 'pips' are observed in the Luders plateau, while more periodic load drops (serrated flow) appear on the flow curve. At still higher temperatures, the serrations in the Luders band regime become higher accompanied by serrations in the flow curve. At about 489 K, the flow curve becomes largely smooth with occasional bands of serrations whereas the serrations still appear in the Luders regime. Finally at 544 K and above, all serrations disappeared with essentially no Luders elongation. The strain rate dependence of the lower critical temperature yielded an activation energy value of ~75 kJ/mol, close to that of carbon and nitrogen diffusion in alpha-iron [11], [14]. Correspondingly athermal regions are observed during the serrated flow (Fig. 2) with essentially temperature and strain-rate independent yield and tensile strengths. Often peaks are noted in the strength in the DSA region indicating negative strain-rate sensitivity with distinct drop in ductility. It is interesting to note here that distinct dips in elongation appear at the lower critical temperature (the onset of serrated yielding) and at the higher critical temperature corresponding to the disappearance of serrations.

Effects of neutron irradiation on load-elongation curves are illustrated in Figures 3a and 3b at ambient temperature and 373 K respectively. We note in Fig. 3a the normally expected radiation hardening with increased strength and embrittlement with decreased elongation to fracture. In addition, Luders strain increased with fluence while essentially rounded yield occurred at the highest fluence with very little elongation. As reported by Murty [1], the lower yield strength and Luders strain increased with cube root of fluence:

$$\Delta\sigma_{LY} \propto (\Phi)^{1/3} \text{ and } \Delta\varepsilon_{LB} \propto (\Phi)^{1/3}, \tag{3}$$

where the subscripts LY and LB stand for lower yield stress and Luders strain respectively while Δ refers to the increase in the lower yield stress and Luders strain following radiation exposure. The cube-root dependence was rationalized on the basis that while the friction hardening (σ_i) in Eq. 1 increases with $\Phi^{1/2}$, the source stress (σ_s) decreases with fluence as will be shown later.

The situation at 373 K is quite different. While radiation hardening is noted following radiation exposure, radiation embrittlement was observed only at the highest fluence of 1.4x10^{19} n/cm^{2}. At all other fluence levels, pronounced increases in ductility are clear. We note that the serrations noted in unirradiated material were suppressed following radiation thereby eliminating or decreasing the embrittlement due to DSA. This is also consistent with the fact that radiation exposure results in decreased source hardening term (or the pinning coefficient). Since the improved ductility at intermediate fluences is accompanied by increased strength, one expects to find increased toughness following irradiation due mainly to the suppression of DSA [15].

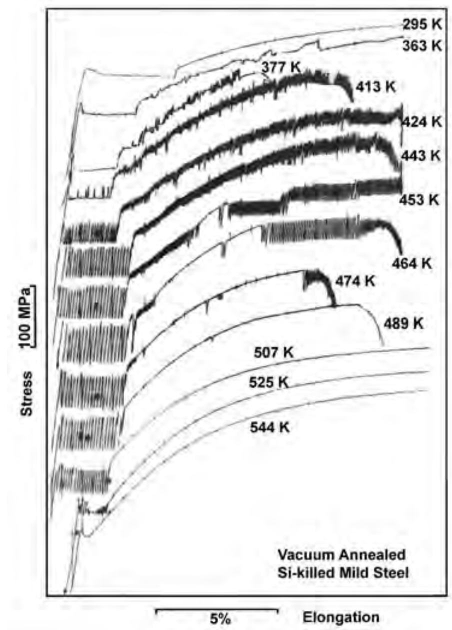

Figure 1. Load-Elongation curves
at different temperatures

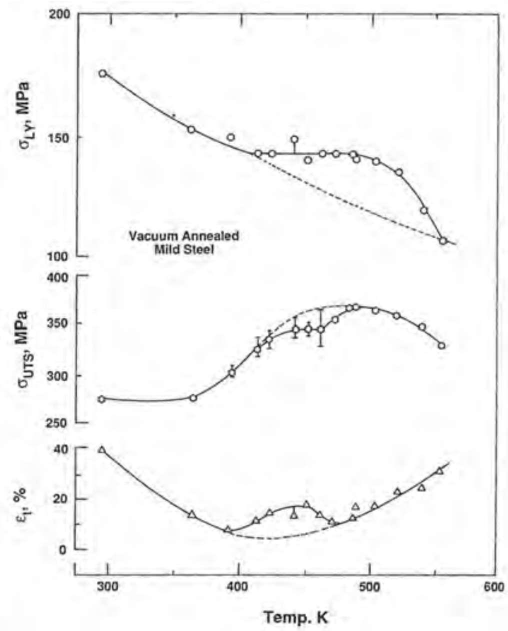

Figure 2. Temperature variation of
yield stress, ultimate tensile strength and total elongation

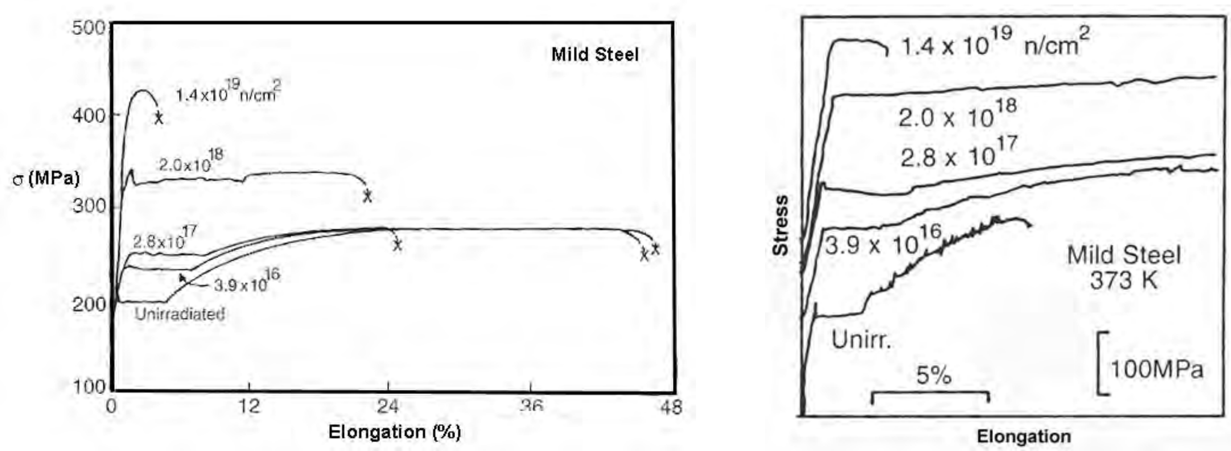

(a) Figure 3 (b)
Effect of neutron irradiation on load-elongation curves at room temperature (a) and 373 K (b)

Effect of test temperature on the load-elongation curves at varied neutron radiation doses was reported by Murty [1] that revealed reduced load drops during DSA, lower critical temperature for the onset of serrations increased with the corresponding decrease in the upper critical temperature for the disappearance. The reduced window of DSA along with the decreased serration height indicates that radiation exposure leads to reduced concentration of interstitial C and N in solution, a fact that was partially verified by internal friction experiments [3] as well as static strain aging tests reported on this mild steel [16]. This also implies that source hardening (σ_s) decreases following radiation exposure. Since grain size dependence of the mechanical properties of mild steel is not available, one needs to apply the Makin-Minter extrapolation technique [1] to evaluate the friction and source hardening terms comprising the yield strength. Such analyses indeed clearly showed that the source hardening decreases with radiation exposure [17] and becomes essentially nil at the highest fluence (10^{19} n/cm^2) that resulted in rounded yield (Fig. 1). This also gave a rationalization for the cube-root dependence of the yield stress on the fluence [1].

The grain size dependence of the yield stress could be investigated on Armco-Fe with grain size varying from 50 μm to 300 μm. The Hall-Petch plots included in Figure 4a indicate that the friction stress (σ_i) in the Hall-Petch equation (Eq. 1) increases while the unpinning coefficient (k_y) decreases following radiation exposure. Radiation exposure to $6.5x10^{17}$ n/cm^2

resulted in a decrease of k_y from 390 to 300 MPa $\sqrt{\mu m}$. This again supports the above contention reached for mild steel that the source hardening term decreases due to radiation exposure (fig. 4b). The temperature variation of σ_s clearly exhibits an increase during DSA indicating the predominant locking of the dislocations by the solute atoms. Correspondingly, the friction hardening exhibited a slight dip during DSA [1].

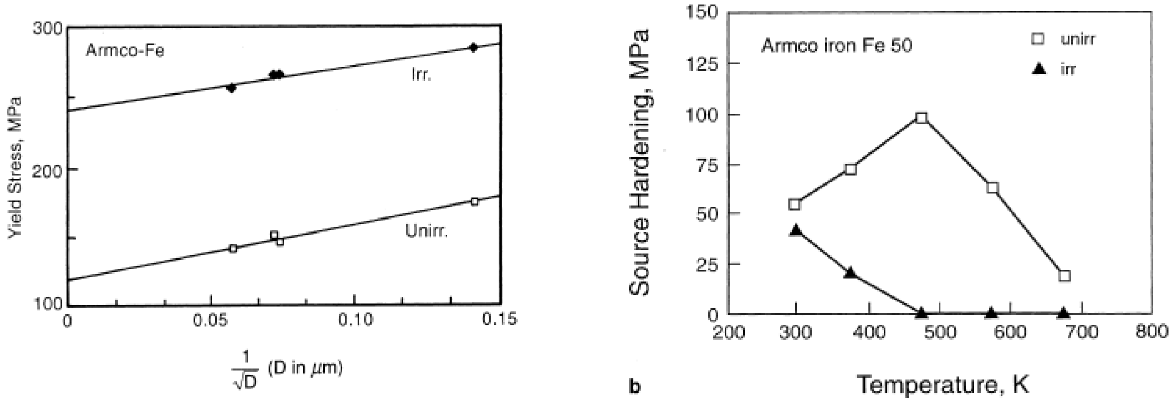

Figure 4
Effect of radiation on Hall-Petch Plot (a) and on temperature variation of σ_s

The effect of low energy (Cd-cutoff) neutrons on the mechanical properties was studied in Armco-iron of different grain sizes and various low alloy steels (Table 1) by some of the samples with Cd-wrapping and some without so that the first set is exposed to fast neutrons only while the unwrapped ones to total neutron flux. A bar chart of the room temperature yield stress is shown in Figure 5 following neutron radiation exposure for 600 hours (2.16×10^6 s) at a fast (> 1 Mev) flux of 1.3×10^{12} n/cm^2/s. It is clear that all alloy steels exhibited slightly higher hardening when exposed to total neutrons while the degree of increase was noted to be a function of the alloy content. It is interesting to note that in pure iron small grain size material exhibited higher strength when exposed to fast neutrons only with a slight decrease following exposure to the whole neutron spectrum. At large grain size ((300 μm) the effect is very similar to that exhibited by alloy steels with a slight increased hardening with no Cd-wrapping. The differences here are small due to the relatively low neutron fluence used in this study.

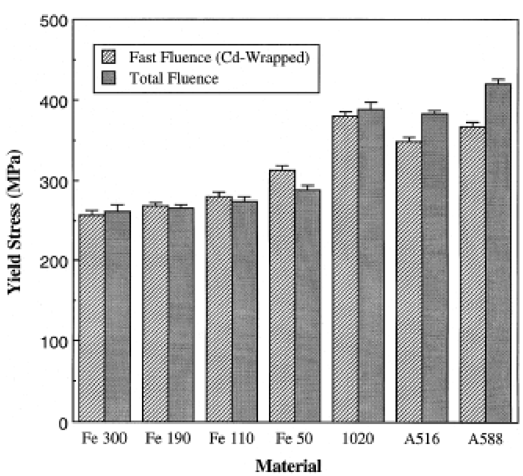

Figure 5
Effect of fast and total neutron irradiation
on yield strength of pure iron and steels

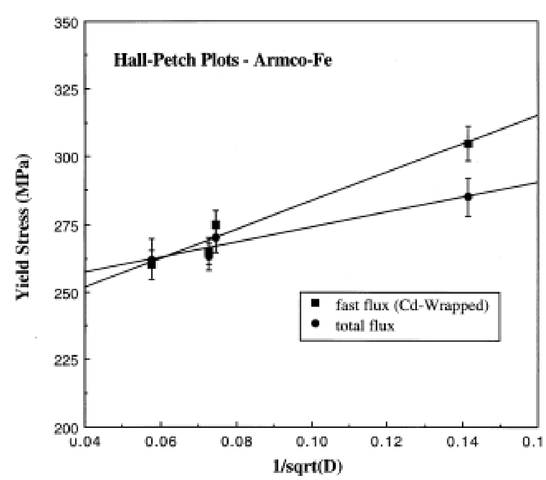

Figure 6
Hall-Petch plots for pure iron depicting
the effect of total vs fast neutron flux

These seemingly contradictory effects can be rationalized on the basis of Hall-Petch plots and the effect of radiation exposure on them (Figure 6). As noted earlier including the data in Figure 4, friction hardening increases with radiation with concomitant decrease in the source hardening or the slope of the Hall-Petch plot. Thus by exposure to the total neutron spectrum (Cd-unwrapped) will result in a slight increase in the strength (y-axis) with decreased slope. Thus the two lines cross making the low grain sized material (extreme right side of x-axis in Fig. 6 weaker when exposed to the total spectrum compared to only fast neutrons. Thus large grain sized materials exhibit the similar trend as for alloy steels. The alloy steels however typically have very small grain size but radiation hardening in these materials is opposite to what has been noted for pure iron. The explanation here is that the source hardening in these steels is relatively very small as indicated by very small yield points and decreased DSA compared to iron and low carbon mild steel. Thus exposure to fast neutrons results in non-aging with σ_s=0 or essentially no slope in the Hall-Petch plot with grain size independent yield strength. By including low energy neutrons the only effect will be an increase in the strength at all grain sizes with the entire strengthening arising from friction hardening (σ_i) only.

SUMMARY AND CONCLUSIONS

Radiation effects were described in pure iron of varied grain sizes, low carbon mild steel and some low alloy steels with emphasis on the synergistic effects of interstitial impurities and radiation defects. The partitioning of the yield strength into friction and source hardening components lends support to the observed phenomena. The grain size dependence of yield strength in iron was noted to follow Hall-Petch relation whose slope decreased following radiation exposure. Importance of source hardening in DSA and radiation effects was pointed out. Influence of low energy (Cd-cutoff) neutrons was evaluated by comparing radiation effects in specimens with and without Cd-wrapping. The resulting radiation hardening was different in pure iron versus alloy steels and the results could be explained using Hall-Petch relation and effect of radiation on it. The significance of source hardening on radiation embrittlement of reactor pressure vessel steels in terms of increased DBTT is brought out.

ACKNOWLEDGEMENTS

This work is supported by the U.S. Department of Energy through the NEER grant DE-FG07-041D14611, and the National Science Foundation grants DMR0412583 and INT0431271.

REFERENCES

1. Murty, K.L., “Role and significance of source hardening in radiation hardening in radiation embrittlement of iron and ferritic steels,” *J. Nuc. Mater.* Vol. 270, 1999, pp. 115-128.
2. Olander, D.R., *Fundamental Aspects of Nuclear Reactor Fuel Elements*, ERDA, Document #TID-26711-P1, 1976.
3. Hall, E.O., *Yield Point Phenomena in Metals and Alloys.* Macmillan, London, 1970.
4. Murty, K.L., “Interstitial-impurity Radiation-Defect Interactions in Ferritic Steels,” *J. Met* October, 1985, pp. 34-39.
5. Wechsler, M.S. and Murty, K.L., “Impurity-Defect Interactions and Radiation Hardening and Embrittlement in BCC Metals,” *Met. Trans.*, Vol. 20A, 1989, pp. 2637-2649.
6. Brauer, G., Liszkay, L., Molnar, B. and Krause, R., “Microstructural aspects of neutron embrittlement of reactor pressure vessel steels - A view from positron annihilation spectroscopy,” *Nucl. Eng. and Design*, Vol. 127, 1991, pp. 47-68.
7. Odette, G.R., “On the dominant mechanism of irradiation embrittlement of reactor pressure vessel steels,” *Scripta Met.*, Vol. 17, 1983, pp. 1183-1187.
8. Hong, J.H., “A Review of the Mechanisms of Radiation Embrittlement of Ferritic Steels,” Report, Electric Power Research Center, North Carolina State University, 1991.
9. Murty, K.L., “Nuclear Materials Research at North Carolina State,” *J. Metals*, Sep., 1985, p. 28.
10. Jung, Y.H. and Murty, K.L., “Effect of Interstitial Impurities on Fracture Characteristics of A533B Class1 Pressure Vessel Steel, *ASTM STP*, Vol. 956, 1987, pp. 395-407.
11. Murty, K.L. and Hall, E.O., “Dynamic Strain Aging and Neutron Irradiation in Mild Steel,” *ASTM STP*, Vol. 611, 1976, pp. 53-71.
12. Srinivas, M., Malakondaiah, G., Linga Murty, K. and Rama Rao, P., “Fracture Toughness in the Dynamic Strain Ageing Regime,” *Scripta Met.* Vol. 25, 1991, pp. 2585-2588.
13. Little, E.A. and Harris, D.R., “The Correlation of Radiation-Hardening with Interstitial Nitrogen Content in Mild Steels,” *Metal Sci. J.* Vol. 4, 1970, pp. 195-202.
14. Charit, I. and Murty, K.L., “Synergistic effects of interstitial impurities and radiation defects on mechanical characteristics of ferritic steels,” *J. Nucl. Mater.,* Vol. 361, 2007, pp. 262-273.
15. Murty, K.L., “Is neutron irradiation always detrimental to metals (iron)?,” *Nature,* Vol. 308, 1984, pp. 51-53.
16. Murty, K.L. and Charit, I., “Static Strain Aging and Dislocation-Impurity Interactions in Irradiated Mild Steel,” presented at the TMS meeting, Orlando, FL , February, 2007.
17. Murty, K.L. and Oh, D.J., “Friction and Source Hardening in Irradiated Mild Steel,” *Scripta Met.* Vol. 17, 1983, pp. 317-320.